Biology Direct

RESEARCH Open Access

Boanmycin overcomes bortezomib resistance by inducing DNA damage and endoplasmic reticulum functional impairment in multiple myeloma

Jin-Xing Wang[1,2,3†], Ling Zhang[4†], Peng-Wei Zhang[1], Luo-Wei Yuan[5], Jian Jiang[1], Xiao-Hui Cheng[1], Wei Zhu[3*], Yong Lei[5*] and Fa-Qing Tian[1*]

Abstract

Background Multiple myeloma (MM) is a hematological malignancy characterized by uncontrolled proliferation of plasma cells and is currently incurable. Despite advancements in therapeutic strategies, resistance to proteasome inhibitors, particularly bortezomib (BTZ), poses a substantial challenge to disease management. This study aimed to explore the efficacy of boanmycin, a novel antitumor antibiotic, in overcoming resistance to BTZ in MM.

Methods BTZ-resistant cells were generated over a period of at least 6 months by gradually increasing the concentration of BTZ. The viability of MM cell lines and patient bone marrow mononuclear cells (BMMCs) was measured via the CCK8 reagent. The protein levels of cleaved caspase 3, cleaved caspase 7, cleaved PARP, PARP, p-JNK, JNK, and γ-H2AX were analyzed through Western blot. Cellular morphology was observed via transmission electron microscopy. Colony formation ability was evaluated, and cell apoptosis and the cell cycle were detected through flow cytometry. Xenograft experiments were conducted to evaluate the growth of MM cells in vivo.

Results Our results demonstrated that boanmycin effectively inhibited cell proliferation and colony formation, and triggered apoptosis in both BTZ-sensitive and BTZ-resistant MM cells. The combination of boanmycin with BTZ had greater inhibitory effects than either drug alone. Furthermore, boanmycin significantly suppressed MM cell growth in immunodeficient mouse xenograft models without inducing distinct toxic side effects. Notably, boanmycin markedly killed patient-derived MM cells ex vivo. Mechanistically, boanmycin not only disrupts the cell cycle and causes DNA damage but also exerts its antitumor effects by inducing endoplasmic reticulum (ER) functional impairment.

†Jin-Xing Wang and Ling Zhang contributed equally to this work.

*Correspondence:
Wei Zhu
zhuwei@gdmu.edu.cn
Yong Lei
leiyong@cuhk.edu.cn
Fa-Qing Tian
trumantfq@163.com

Full list of author information is available at the end of the article

Conclusions Our findings highlight the potential of boanmycin as a promising novel therapeutic option for treating MM, particularly in patients with BTZ resistance.

Keywords Multiple myeloma, Boanmycin, Bortezomib resistance, Endoplasmic reticulum

Background

Multiple myeloma (MM) is an aggressive hematological malignancy characterized by the abnormal growth of plasma cells [1]. The incidence of MM is significantly greater among older individuals, with a median age of approximately 70 years [2]. MM patients experience distressing symptoms such as anemia, renal injury, infections, hypercalcemia and bone disease [1]. Despite advancements in medical treatment that have extended patient survival, MM remains incurable [3]. Bortezomib, a selective proteasome inhibitor, has shown remarkable efficacy in MM treatment when combined with immunomodulatory drugs such as lenalidomide and pomalidomide, corticosteroids such as dexamethasone, and/or a monoclonal antibody such as daratumumab [4]. However, the effectiveness of BTZ is limited due to the development of drug resistance [5]. Although other proteasome inhibitors, such as carfilzomib and ixazomib, can partially overcome BTZ resistance, BTZ remains a critical first-line treatment for MM [6]. Therefore, strategies to overcome BTZ resistance are highly valuable.

Boanmycin, a novel antitumor antibiotic, has been used primarily for treating head and neck squamous cell carcinoma [7]. Preclinical experiments have illustrated the efficacy of boanmycin against various types of cancer, including hepatocellular carcinoma, colorectal cancer, and colon cancer [7–9]. A phase I clinical study revealed that boanmycin induces minimal bone marrow suppression and exhibits lower pulmonary toxicity than bleomycin and pingyangmycin [9]. A phase II clinical study involving a cohort of 325 patients with intermediate and malignant carcinoma demonstrated the therapeutic potential of boanmycin in treating malignant lymphoma, head and neck cancer, breast cancer, and esophageal cancer while causing limited bone marrow suppression and functional impairment of the liver or kidney [10]. Moreover, researchers have developed a temperature-sensitive boanmycin in situ gel that can successfully prolong the release of boanmycin and enhance its antitumor properties in the treatment of liver cancer [11]. Ding et al. also formulated an in situ gel system incorporating anionic liposomes loaded with boanmycin to augment its cytotoxic effects [8].

The endoplasmic reticulum (ER) is a crucial organelle responsible for protein synthesis, folding, and modification [12, 13]. Additionally, the ER is the main intracellular reservoir for Ca^{2+} and is crucial for maintaining Ca^{2+} homeostasis through interactions with other organelles and the plasma membrane [14]. Perturbations in cellular homeostasis caused by internal or external factors can lead to ER stress [15]. Targeting the ER signaling pathway holds promise for anticancer therapy, as certain reagents can selectively induce or inhibit ER stress, thereby hindering the proliferation and survival of cancer cells [16]. Multiple myeloma cells are particularly susceptible to proteotoxicity due to the overproduction of paraproteins [17], making the ER signaling pathway a potential target for MM treatment.

Currently, there is limited research on the use of boanmycin and other bleomycin derivatives for treating hematologic malignancies. Previous investigations have illustrated the capacity of bleomycin to induce mitochondrial DNA damage in AML cells, leading to cellular apoptosis [18]. The efficacy of boanmycin in BTZ-resistant MM cells remains unexplored. Boanmycin exerts its effects by inhibiting protein synthesis, suggesting its potential utility in MM treatment [19]. Here, we demonstrated that boanmycin inhibits the proliferation and colony formation of both BTZ-sensitive and BTZ-resistant MM cells. Additionally, we elucidated the mechanism by which boanmycin triggers DNA damage and impairs ER function to induce cell death. Our findings suggest the promising pharmacological utility of boanmycin in the management of MM, particularly in cases of BTZ resistance.

Materials and methods

Cells and reagents

Multiple myeloma cell lines, RPMI 8226, U266B1 and MM.1 S, were obtained from the American Type Culture Collection (ATCC) and cultured in RPMI 1640 medium supplemented with 10% fetal bovine serum (FBS). Bone marrow mononuclear cells (BMMCs) were collected from MM patients. The Fluo-4 AM probe and the CellTrace™ CFSE kit were purchased from Thermo Fisher Scientific (MA, USA). The cell cycle analysis kits and ER-Tracker dye were purchased from Beyotime Company (Shanghai, China). The CCK8 reagent, Annexin V/PI apoptosis analysis reagent kit, and highly sensitive ECL solution were purchased from Vazyme Company (Nanjing, China). The methylcellulose stock solution was purchased from R&D Systems (MN, USA). Boanmycin was a gift from Jilin AoDong Pharmaceutical Group Company (Jilin, China) and was dissolved in PBS at a concentration of 100 mg/mL as a stock solution. The apoptosis antibody sampler kit was purchased from Cell Signaling Technology (MA, USA).

Cell viability assay

For the MM cell lines, 10,000 cells per well were seeded in a 96-well plate, while patient-derived primary cells were seeded at a density of 20,000 cells per well. The cells were subjected to treatment with various concentrations of boanmycin for 48 h or with the indicated concentrations of boanmycin for different time intervals. Subsequently, 10 μL of CCK8 reagent was added, and the plate was subjected to a 4-hour incubation at 37 °C in a 5% CO_2 incubator. Absorbance readings were obtained at a wavelength of 450 nm via a Spark microplate reader (TECAN, Austria).

CFSE staining assay

The cells were incubated with carboxyfluorescein succinimidyl ester (CFSE) at a final concentration of 5 μM for 30 min at 37 °C in an incubator. The cells were subsequently washed twice with RPMI 1640 medium and then subjected to treatment with various concentrations of boanmycin for 48 h. Following this treatment, the cells were collected, washed, and resuspended in RPMI 1640 medium. CFSE fluorescence was assessed via flow cytometry and analyzed using FlowJo software (CytoFLEX, Beckman Coulter, CA, USA).

Wright-Giemsa staining

The collected cells were washed and resuspended in phosphate buffered saline (PBS). A total of 100 μL of cell suspension containing 100,000 cells was carefully spun onto glass slides. The cells were then fixed with 70% ethanol for 10 min. Following fixation, the cells were stained with a modified Giemsa staining solution and subsequently observed under an inverted microscope (BDS400, CNOPTEC, Chongqing, China) for imaging.

Colony formation assay

A total of 200 cells were cultured in each well of a 24-well plate, with medium comprising 0.9% methylcellulose combined with varying concentrations of boanmycin (0, 0.4, and 0.8 μg/mL). Following an incubation period of approximately two weeks, the resulting colonies were enumerated and imaged via an inverted microscope (BDS400, CNOPTEC, Chongqing, China).

Apoptosis analysis

The harvested cells were subjected to different concentrations of boanmycin (0, 20, 40, and 60 μg/mL) for 48 h. Following this, the cells were collected by centrifugation at 1800 rpm for 5 min and washed twice with PBS. The cells were subsequently incubated with annexin V/propidium iodide (PI) dye for 10 min at room temperature. Apoptosis analysis was then performed according to the manufacturer's instructions for the annexin V/PI apoptosis analysis kit.

Cell cycle analysis

Briefly, the cells were treated with various concentrations of boanmycin for 48 h. After treatment, the cells were collected and washed with precooled PBS twice. The cells were subsequently resuspended in precooled 70% ethanol and fixed at 4 °C overnight. Then, the cells were washed twice with PBS and stained according to the instructions provided with the cell cycle analysis kit. Cell cycle analysis was performed via flow cytometry, and the data were analyzed with FlowJo software.

Cellular Ca^{2+} level determination

The cells were exposed to a designated concentration of boanmycin (0, 20, 40, and 60 μg/mL) for 48 h. Subsequently, the cells were collected, rinsed twice with PBS (without Ca^{2+} and Mg^{2+}), and exposed to 2 μM Fluo-4 AM for 30 min at 37 °C in the dark. The intracellular calcium levels were assessed via flow cytometry (CytoFLEX, Beckman Coulter, CA, USA).

ER-tracker staining assay

The ER-Tracker working solution was prepared by diluting the stock solution with RPMI 1640 medium at a ratio of 1:1000. Following the treatment of the cells with specified concentrations of boanmycin for 48 h, the cells were collected, rinsed twice with RPMI 1640 medium, and exposed to 100 μL of ER-Tracker working solution for 30 min at 37 °C in the dark. The cells were subsequently washed twice and analyzed via flow cytometry (CytoFLEX, Beckman Coulter, CA, USA).

Quantitative real-time PCR

Briefly, the collected cells were washed with PBS and lysed with TRIzol reagent (Invitrogen Life Technologies, Carlsbad, CA, USA). Total RNA was isolated and reverse transcribed to cDNA via the HiScript II 1st Strand cDNA Synthesis Kit (Vazyme, Nanjing, China). The mRNA expression levels were quantified using the QuantStudio Real-Time PCR System (Applied Biosystems, Foster City, CA, USA), with normalization to the GAPDH gene.

Western blot analysis

The cells were collected and incubated in RIPA buffer at 4℃ for 20 min. The resulting cell lysates were centrifuged, and the supernatants were combined with protein loading buffer and incubated at 100℃ for 5 min. Subsequently, the protein samples were separated by SDS-PAGE and then transferred to nitrocellulose membranes. The membranes were then blocked with 5% BSA buffer for 1 h and subjected to overnight incubation at 4℃ with antibodies against cleaved caspase 3 (#9964), cleaved caspase 7 (#8438), cleaved PARP (#5625), and PARP (#9542). Then, the membranes were incubated with a peroxidase-conjugated goat anti-rabbit secondary antibody (#7074)

for 1 h. Antibody binding was detected through an enhanced chemiluminescence solution and Chemidoc imaging system (Bio-Rad, Milan, Italy).

Transmission electron microscopy (TEM)

The cells were first collected and fixed overnight at 4℃ via TEM fixation buffer. Subsequently, the fixed cells were centrifuged, resuspended, and washed three times with phosphate buffer. Next, the cells were embedded in a 1% agarose solution. The agarose blocks were then fixed with 1% OsO4 for 2 h at room temperature. Dehydration was carried out using various concentrations of alcohol and acetone. The blocks were further infiltrated and embedded with resin before being transferred to an oven set at 65℃ for a minimum of 48 h to undergo polymerization. The resin blocks were cut into thin sections of 60–80 nm using an ultramicrotome, and the tissues were carefully placed onto 150-mesh cuprum grids with formvar film. After being stained with a 2% uranium acetate-saturated alcohol solution and 2.6% lead citrate, the samples were observed via a Hitachi transmission electron microscope (Tokyo, Japan).

Bioinformatic analysis

Total RNA was extracted using the TRIzol reagent. The RNA samples were reverse transcribed and then sequenced via the Illumina HiSeq2500 platform. Differentially expressed genes (DEGs) were identified by DESeq2 software. All DEGs were subjected to analysis using the Gene Ontology (GO) database (http://www.geneontology.org/) and the Kyoto Encyclopedia of Genes and Genomes (KEGG) pathway database (https://www.genome.jp/kegg/). Furthermore, gene set enrichment analysis (GSEA) was performed via GSEA software to determine significant differences in a set of genes within specific GO terms, KEGG terms, or disease ontology (DO) terms between the two groups. Enrichment scores and *p*-values were calculated via the default parameters.

Animal study

Six-week-old female BALB/c-nu and NOD-SCID mice were procured from Beijing Vital River Laboratory Animal Technology Company. Each BALB/c-nu mouse received a subcutaneous injection of 4×10^5 RPMI 8226 or RPMI 8226-Res cells into the flank. Similarly, each NOD-SCID mouse was injected subcutaneously with 1×10^6 MM.1 S cells into the flank. Approximately one week later, once the tumors became palpable, the mice were administered either PBS (Vehicle, $n=5$) or 10 mg/kg boanmycin (BAM, $n=5$) intraperitoneally every three days. Once the tumors reached a predetermined size, the mice were euthanized, and the tumors were excised, weighed, and fixed in 4% paraformaldehyde for subsequent immunohistochemical analysis. Tumor volumes were determined using calipers and calculated according to the formula: $A\times B^2/2$, where A denotes the longest diameter and B represents the diameter perpendicular to A. Furthermore, the body weight, feeding behavior, and motor activity of each animal were monitored as indicators of general health. All animal care and experimental procedures were approved by the Institutional Animal Care and Use Committee of The Chinese University of Hong Kong (Shenzhen) (No. CUHKSZ-AE2021011), following the WMA statement on animal use in biomedical research.

Immunohistochemistry

Tumors from the mice were fixed in 4% paraformaldehyde. Sections with a thickness of 4 μm were prepared, deparaffinized, and subsequently rehydrated using xylene and a series of graded ethanol solutions. After washing with PBS and antigen retrieval, the sections were blocked with 10% normal rabbit serum at room temperature for 1 h. Then, the sections were incubated overnight at 4 ℃ with a rabbit anti-Ki-67 antibody. The slides were incubated with a peroxidase-conjugated secondary antibody for 1 h at room temperature, followed by treatment with diaminobenzidine and observation via microscopy. For hematoxylin-eosin (HE) staining, the slides were separately stained with hematoxylin and eosin, and observed after they were sealed with neutral gum.

Statistical analysis

All the data were analyzed with GraphPad Prism 6 software. The results are expressed as the mean ± SD of three independent experiments. *P* values were determined by ANOVA for multiple comparisons or unpaired *t*- tests for two-group comparisons. A *p*- value less than 0.05 was considered significant and is indicated by asterisks (*).

Results

Boanmycin inhibits proliferation and induces apoptosis in multiple myeloma cells

Boanmycin, an anti-tumor antibiotic, has not been clinically utilized in the treatment of multiple myeloma (MM). To assess the inhibitory effects of boanmycin on MM, RPMI 8226, U266B1, and MM.1 S cells were treated with varying concentrations and durations of boanmycin, and the cell viability was subsequently measured using the CCK8 reagent. These findings indicated that boanmycin effectively impeded the growth of MM cells in a dose- and time-dependent manner (Fig. 1A). The IC_{50} values of boanmycin in RPMI 8226, U266B1, and MM.1 S cells were 17.49, 29.05, and 13.89 μg/mL, respectively (Supplementary Fig. 1A). Additionally, Wright–Giemsa staining was performed on RPMI 8226 and U266B1 cells. As shown in Fig. 1B, treatment with boanmycin resulted in an increase in cell and nuclear size, an increase in

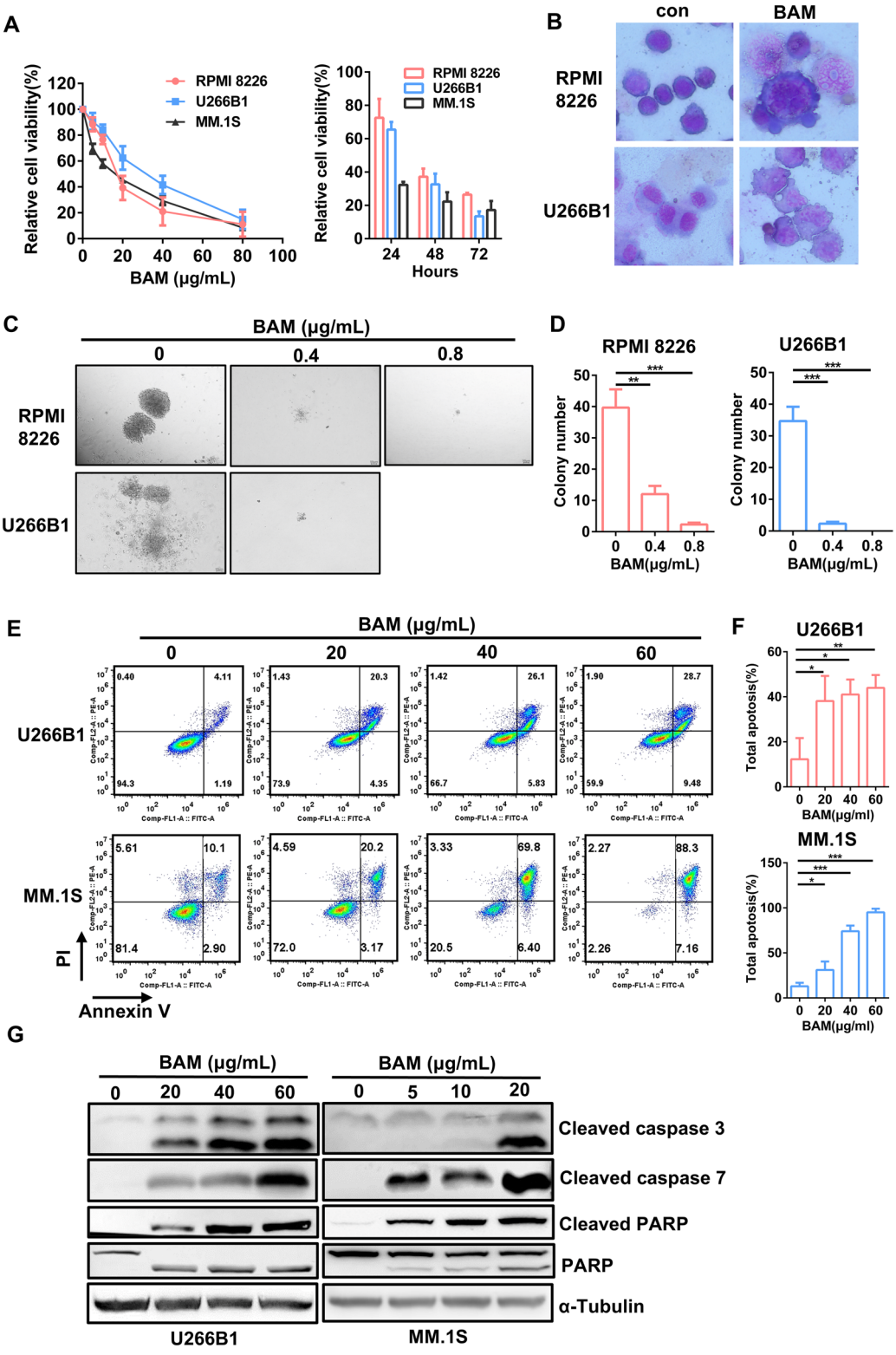

Fig. 1 Boanmycin inhibits cell proliferation and induces cell apoptosis in multiple myeloma cells. (**A**) RPMI 8226, U266B1, and MM.1 S cells were exposed to varying concentrations and durations of boanmycin, after which the relative cell viability was assessed using the CCK8 reagent. (**B**) Cell morphology was evaluated through Wright-Giemsa staining with and without boanmycin treatment. (**C**) RPMI 8226 and U266B1 cells were treated with 0, 0.4 and 0.8 μg/mL of boanmycin for approximately 15 days, after which the colonies were photographed, and (**D**) the number of colonies was counted. (**E**) Apoptosis analysis was performed via flow cytometry using Annexin V/PI staining, and (**F**) the proportion of total apoptotic cells was determined. (**G**) Western blot analysis of PARP, cleaved PARP, cleaved caspase 3, and cleaved caspase 7 in MM cells treated with boanmycin for 48 h. α-Tubulin served as a control. (mean ± SD, $^{*}p < 0.05$, $^{**}p < 0.01$ and $^{***}p < 0.001$)

the number of cytoplasmic vacuoles, and the presence of abnormal folds in the cell membrane. Furthermore, boanmycin significantly inhibited colony formation ability of MM cells, as evidenced by a substantial reduction in both the number and size of colonies. Notably, when the concentration of boanmycin exceeded 0.8 μg/mL, there was a pronounced impairment in colony formation in RPMI 8226 cells, and no colonies were observed in U266B1 cells (Fig. 1C and D). We also demonstrated that boanmycin induced G2/M phase cell cycle arrest in MM cells (Supplementary Fig. 1B). The exposure of the MM cells to boanmycin significantly increased the proportion of apoptotic cells (Fig. 1E and F). Additionally, the results of the immunoblot assay revealed a visible increase in the levels of cleaved PARP, cleaved caspase 3 and cleaved caspase 7 after boanmycin treatment for 48 h (Fig. 1G). Boanmycin also elicited DNA damage, as indicated by elevated γ-H2AX protein levels (Supplementary Fig. 2D). These findings demonstrated that boanmycin effectively inhibits the proliferation and induces the apoptosis of MM cells.

Boanmycin enhances the inhibitory effect of BTZ on multiple myeloma cells

BTZ is a first-line drug for the treatment of MM [4]. To investigate the inhibitory effect of combining boanmycin and BTZ, we incubated MM cells with different concentrations of BTZ (0, 2, 4, 6, 8 and 10 nM) and boanmycin (20 μg/mL for U266B1 cells, 10 μg/mL for MM.1 S cells) for 48 h, and cell viability was evaluated using the CCK8 reagent. Our results demonstrated that boanmycin significantly enhanced the inhibitory effect of BTZ on U266B1 and MM.1 S cells (Fig. 2A). Compared with each drug alone, the combination of boanmycin and BTZ resulted in further increases in the levels of apoptotic proteins (Fig. 2B). Flow cytometry experiments revealed that the combination of the two drugs induced apoptosis to a greater extent (Fig. 2C). Overall, the combination of boanmycin and BTZ exhibited enhanced inhibitory effects and led to increased levels of apoptosis.

The inhibition of BTZ-resistant multiple myeloma cells by boanmycin

Resistance to BTZ remains a challenge in the treatment of MM. To investigate whether boanmycin can overcome BTZ resistance, we established the BTZ-resistant cell strains RPMI 8226-Res and U266B1-Res by gradually increasing the concentration of BTZ in the culture medium for at least 6 months. The successful construction of the resistant cell strains was confirmed by cell viability assays (Fig. 3A). Next, we treated MM cells, including BTZ-resistant cell strains, with various concentrations of boanmycin. The results of the CFSE assays revealed that boanmycin significantly inhibited the proliferation of BTZ-resistant MM cells (Fig. 3B). Moreover, boanmycin inhibited the colony formation of BTZ-resistant MM cells (Fig. 3C and D). The western blot assay was subsequently performed to evaluate the apoptosis signaling induced by boanmycin. The levels of proteins associated with the canonical apoptosis pathway increased upon boanmycin treatment (Fig. 3E). Furthermore, flow cytometry assays demonstrated that boanmycin significantly induced the death of BTZ-resistant MM cells (Fig. 3F). Therefore, boanmycin had favorable inhibitory effects on BTZ-resistant MM cells.

Bioinformatics analysis of boanmycin-induced signaling pathway changes in multiple myeloma cells

To evaluate the impact of boanmycin on signaling pathways in MM cells, we conducted RNA sequencing analysis on the boanmycin-treated and control groups. Our study revealed that boanmycin treatment led to the upregulation of 873 genes and the downregulation of 103 genes, as determined by a log2 fold change greater than 1 (Fig. 4A and B). Additionally, we performed Gene Ontology (GO) and Kyoto Encyclopedia of Genes and Genomes (KEGG) pathway analyses, which revealed enrichment of pathways associated with cell apoptosis, DNA damage, and cell cycle signaling (Fig. 4C and D and Supplementary Fig. 2A, B). Furthermore, boanmycin downregulated the c-MYC pathway and upregulated the P53 pathway (Supplementary Fig. 2C, E). We also observed enrichment of pathways related to ER function and calcium signaling (Fig. 4C and D). Gene set enrichment analysis (GSEA) revealed the downregulation of pathways involved in the cell cycle and DNA replication (Fig. 4E). GSEA lollipop plots demonstrated the upregulation of pathways associated with calcium ion binding, the ER lumen, and the MAPK cascade (Fig. 4F). These findings suggest that boanmycin not only inhibits the cell cycle and induces cell apoptosis but also leads to alterations in ER function in MM cells.

Boanmycin induces endoplasmic reticulum functional impairment in multiple myeloma cells

GSEA revealed the upregulation of pathways related to ER function and the calcium signaling pathway in the boanmycin-treated groups (Fig. 5A). Furthermore, the combination of boanmycin and BTZ increased the expression of the CHOP gene, a key regulator of ER stress (Fig. 5B). To visualize the impact of boanmycin on organelle morphology, we employed the transmission electron microscopy assay, which revealed an irregular arrangement and elongation of the ER in the boanmycin-treated cells (Fig. 5C). Additionally, RPMI 8226-Res and U266B1-Res cells were treated with various concentrations of boanmycin (0, 20, 40, 60 μg/mL) for 48 h and stained with ER-Tracker dye. The results demonstrated

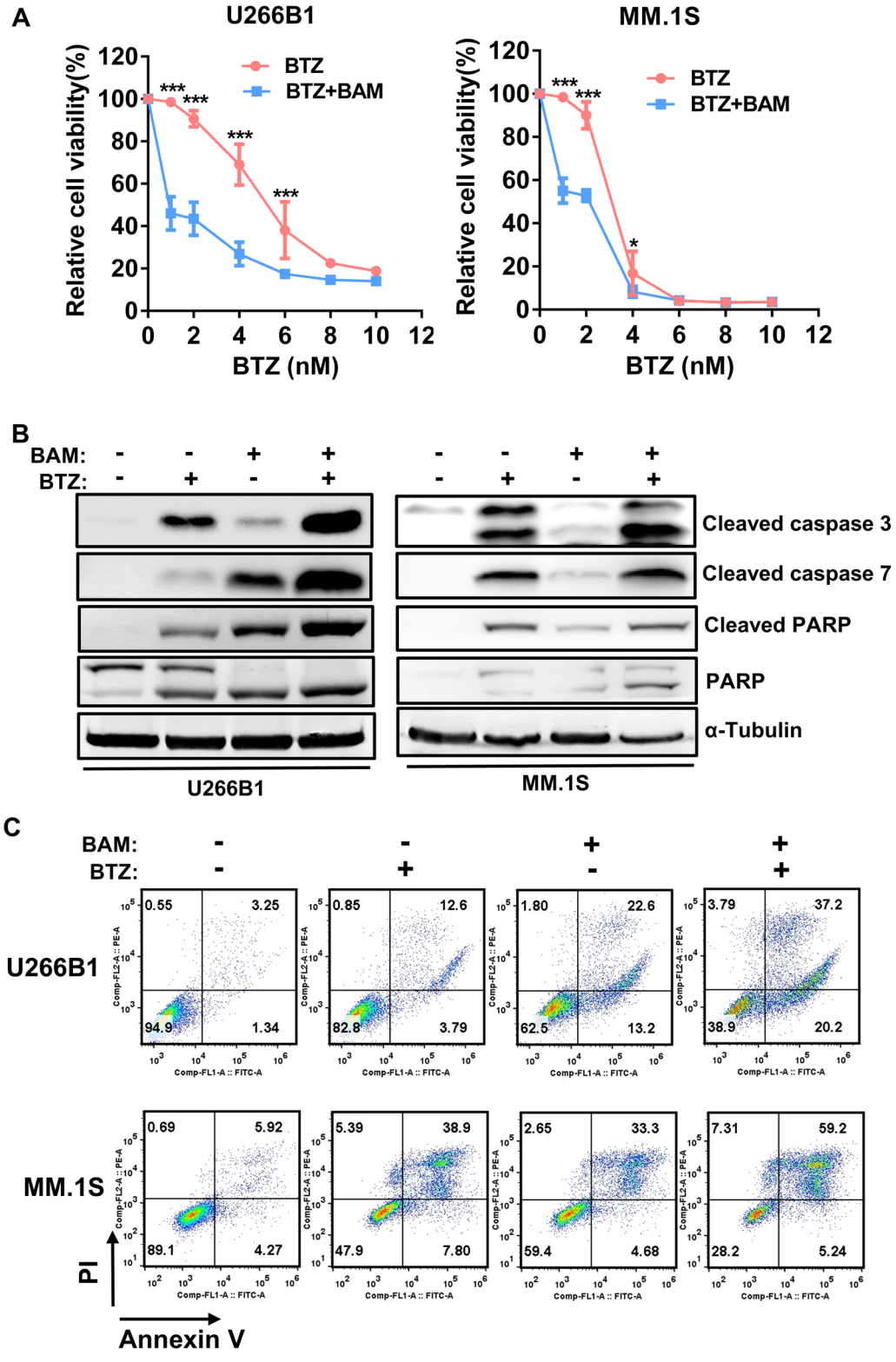

Fig. 2 Boanmycin enhances the inhibitory effect of BTZ in multiple myeloma cells. (**A**) The relative viability of U266B1 and MM.1 S cells treated with different concentrations of BTZ and boanmycin for 48 h was determined. (**B**) Western blot analysis was conducted on PARP, cleaved PARP, cleaved caspase 3 and cleaved caspase 7 proteins after the cells were treated with BTZ and/or boanmycin for 48 h. α-Tubulin was used as a control. (**C**) Apoptosis analysis was performed via flow cytometry using Annexin V/PI staining. (mean ± SD, $*p < 0.05$, $**p < 0.01$ and $***p < 0.001$)

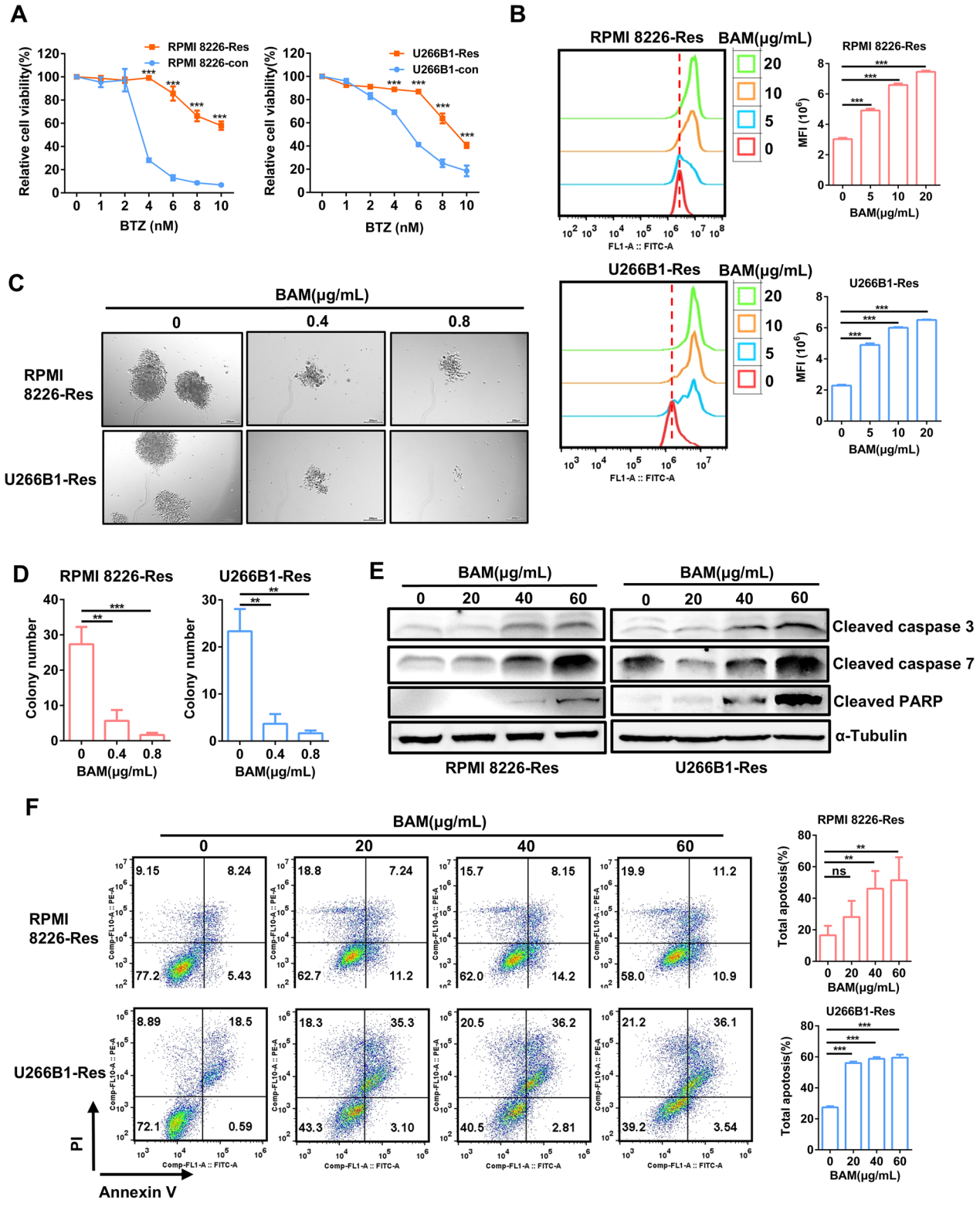

Fig. 3 The inhibitory effect of boanmycin on BTZ-resistant multiple myeloma cells. (**A**) The cell viability assay was conducted to evaluate the sensitivity of RPMI 8226-Res and U266B1-Res cells, as well as the corresponding parental cell lines to BTZ. (**B**) The inhibitory effects of boanmycin on BTZ-resistant MM cells were assessed through CFSE staining. (**C**) Colonies were photographed and (**D**) counted after incubation of RPMI 8226-Res and U266B1-Res cells with different concentrations of boanmycin for 15 days. (**E**) Western blot analysis of proteins associated with cell apoptosis. (**F**) The level of apoptosis induced by boanmycin in BTZ-resistant MM cells was determined by flow cytometry. (mean ± SD, *$p < 0.05$, **$p < 0.01$ and ***$p < 0.001$)

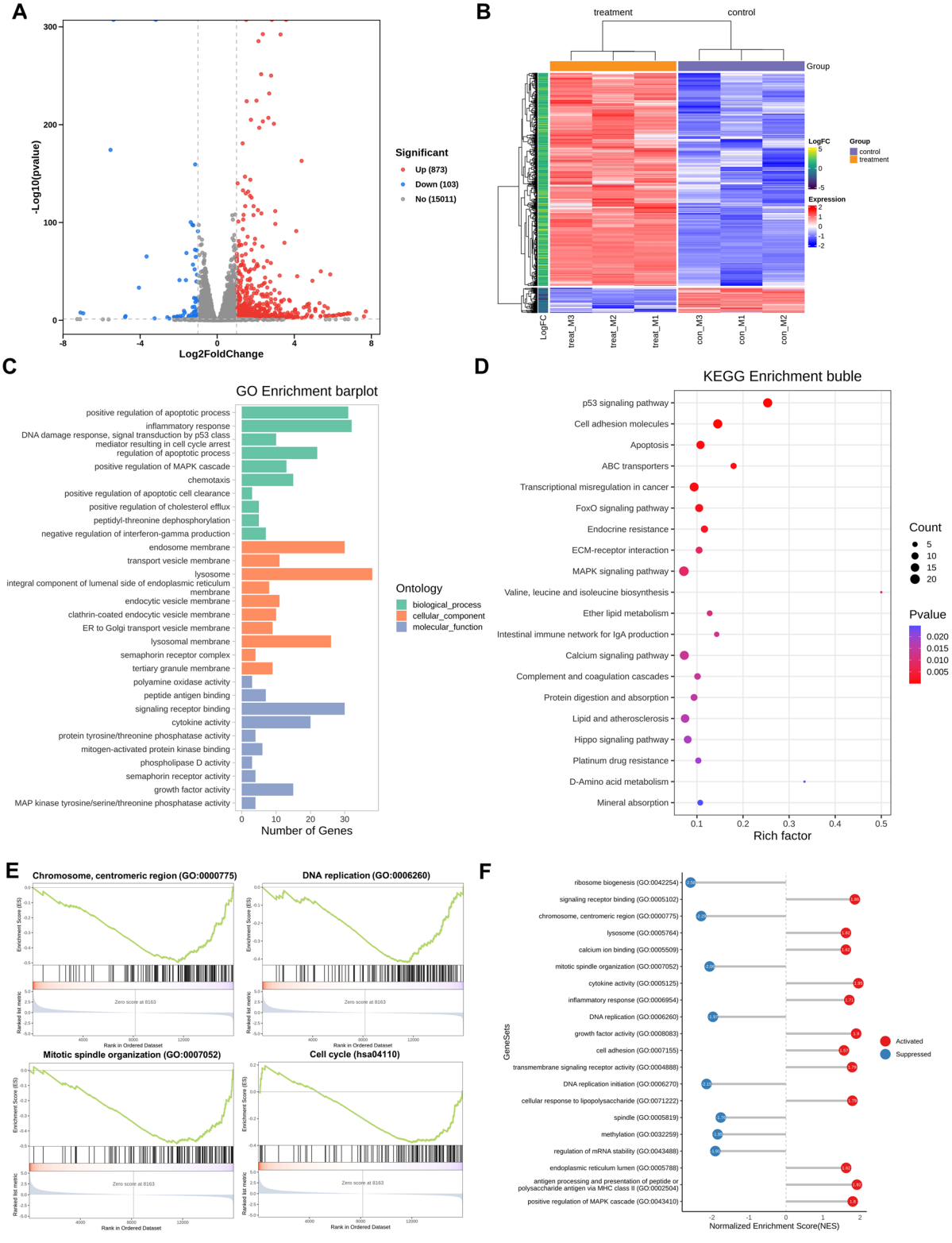

Fig. 4 Bioinformatics analysis of boanmycin-induced signaling pathway changes in multiple myeloma cells. (**A**) A volcano map was generated to visualize significantly differentially expressed genes. Red spots indicate upregulated genes, whereas blue spots indicate downregulated genes. (**B**) A heatmap was created to display the differential expression of genes between the control and boanmycin-treated groups. (**C**) The differentially expressed genes (DEGs) were subjected to Gene Ontology (GO) analysis for biological processes (BP), cellular components (CC), and molecular functions (MF). (**D**) The differentially expressed genes were analyzed via the KEGG database for signaling pathway analysis. (**E**) Gene set enrichment analysis (GSEA) was performed. (**F**) GSEA lollipop plots were generated to illustrate the upregulated or downregulated pathways based on the GO database

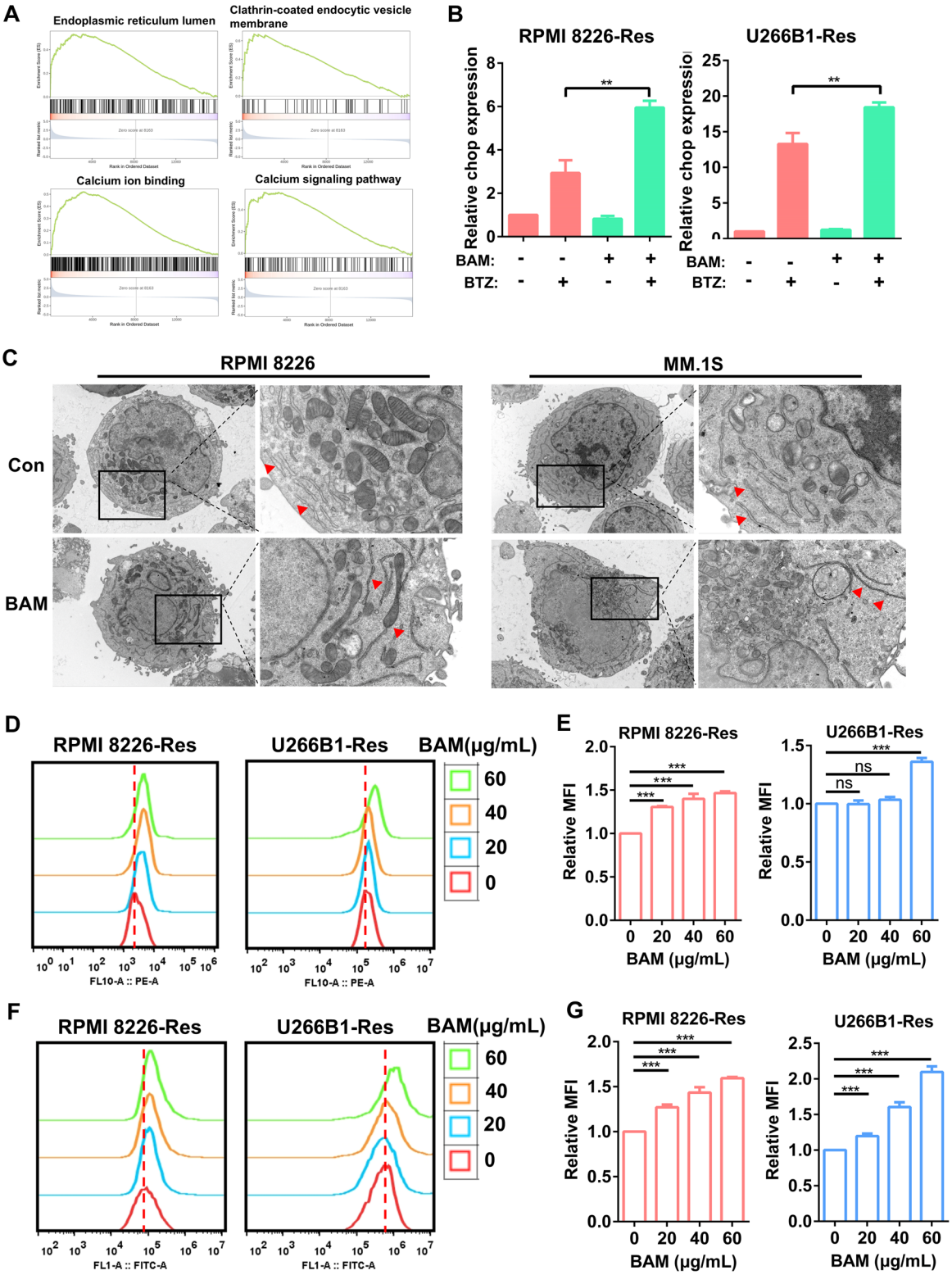

Fig. 5 Boanmycin induces endoplasmic reticulum functional impairment in multiple myeloma cells. (**A**) GSEA was conducted to analyze the enrichment of signaling pathways associated with ER function. (**B**) qPCR assays were performed to quantify the relative expression of the CHOP gene after the cells were treated with bortezomib and/or boanmycin. (**C**) After incubation with boanmycin for 48 h, RPMI 8226 and MM.1 S cells were fixed and subjected to TEM to observe their intracellular morphology. (**D**) RPMI 8226-Res and U266B1-Res cells treated with different concentrations of boanmycin for 48 h were stained with ER-Tracker dye, and (**E**) the relative mean fluorescence intensity (MFI) was calculated and plotted. (**F**) RPMI 8226-Res and U266B1-Res cells treated with different concentrations of boanmycin for 48 h were stained with a Fluo 4-AM probe, and (**G**) the relative MFI was calculated and plotted. (mean ± SD, $*p < 0.05$, $**p < 0.01$ and $***p < 0.001$)

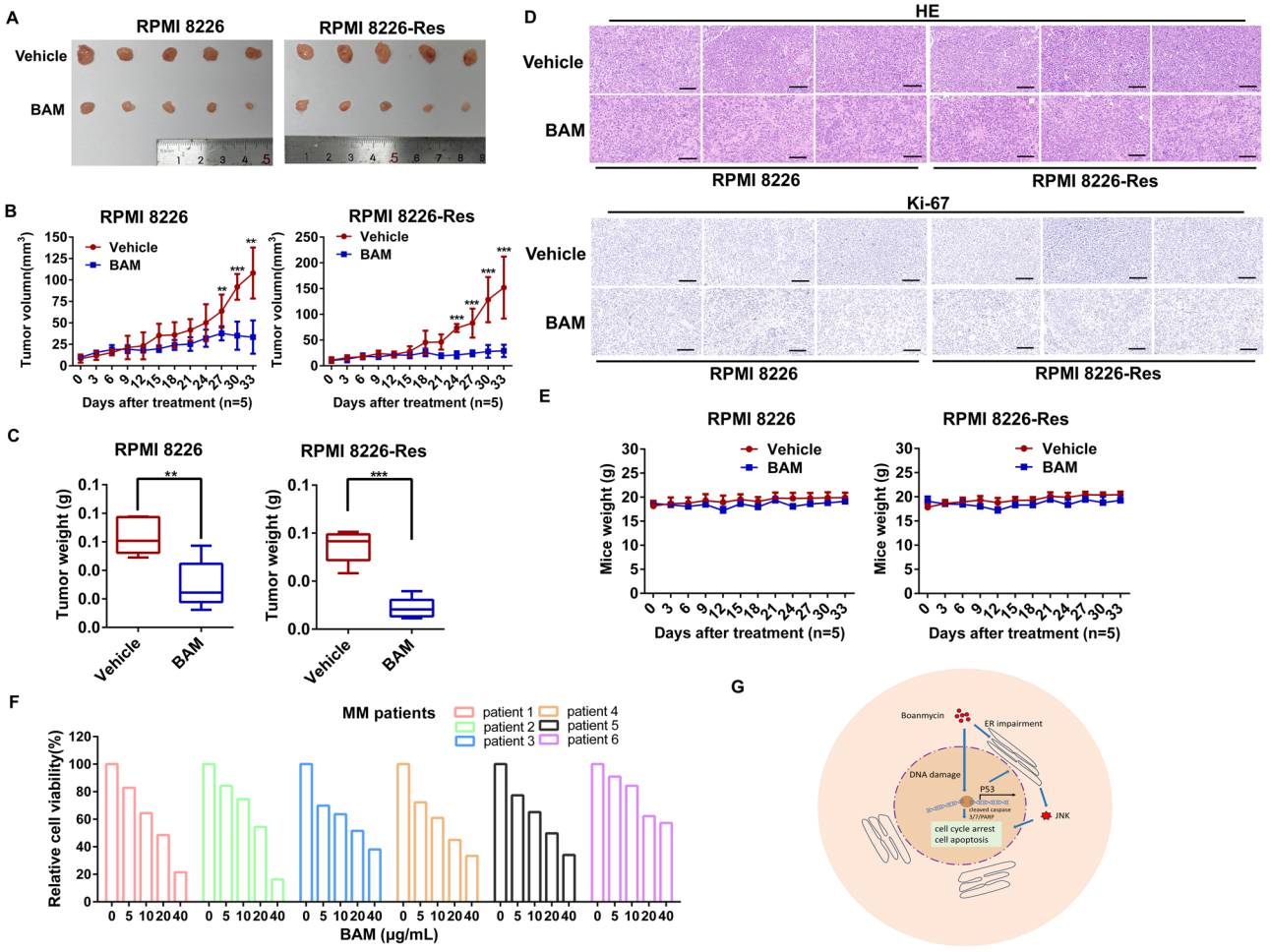

Fig. 6 Boanmycin inhibits the growth of multiple myeloma cells in mouse xenograft models and patient samples. (**A**) BALB/c-nu mice bearing RPMI 8226 or RPMI 8226-Res xenografts were treated with vehicle (PBS) or 10 mg/kg boanmycin every three days for 33 days. Photographs of tumors separated from animals are presented ($n = 5$ mice per group). (**B**) The tumor volumes were monitored and plotted over the indicated time (n = 5 mice per group). (**C**) The tumor weights of sacrificed animals were analyzed and plotted (n = 5 mice per group). (**D**) Hematoxylin and eosin (HE) staining and Ki-67 immunohistochemical staining of the xenografts were performed ($n = 3$ mice per group). (**E**) Body weight changes were plotted versus time ($n = 5$ mice per group). (**F**) Determination of the viability of BMMCs treated with different concentrations of boanmycin for 48 h. (**G**) Scheme by which boanmycin eradicates MM cells: Boanmycin disrupts the cell cycle and induces apoptosis by damaging DNA and triggering ER impairment in multiple myeloma cells. (mean ± SD, $^{*}p < 0.05$, $^{**}p < 0.01$ and $^{***}p < 0.001$ vs. vehicle)

that boanmycin enhanced probe signaling and the relative mean fluorescence intensity (Fig. 5D and E). By using the Fluo-4 AM probe to label calcium ions, we observed a substantial increase in cytoplasmic calcium levels following boanmycin treatment (Fig. 5F and G). Considering that calcium is primarily stored in the ER [20], we concluded that boanmycin induced functional impairment of the ER in MM cells.

Boanmycin inhibits the growth of multiple myeloma cells in mouse xenograft models and patient samples

To investigate the effects of boanmycin in vivo, xenograft models were established by injecting 4×10^5 RPMI 8226 or RPMI 8226-Res cells into the flanks of each BALB/c-nu mouse. Similarly, 1×10^6 MM.1 S cells were injected into the flanks of each NOD-SCID mouse. Compared with the vehicle-treated groups, the groups treated with boanmycin presented significantly reduced tumor sizes, suggesting the inhibitory impact of boanmycin on tumor growth (Fig. 6A; Supplementary Fig. 3A). Furthermore, both the tumor volume and weight were notably lower in the boanmycin-treated groups than in the vehicle-treated groups (Fig. 6B and C; Supplementary Fig. 3B, C). Importantly, no significant fluctuations in body weight were observed in either the boanmycin-treated groups or the vehicle-treated groups, indicating a low toxicity profile of boanmycin (Fig. 6E; Supplementary Fig. 3D).

Histological examination through hematoxylin and eosin (HE) staining revealed a marked increase in both cellular and nuclear sizes, along with a greater proportion

of multinucleated cells in tumors subjected to boanmycin treatment. Cell proliferation, as measured by Ki-67 expression, was lower in the boanmycin-treated groups than in the vehicle-treated groups (Fig. 6D; Supplementary Fig. 3E). Additionally, HE staining revealed no discernible alterations in the tissue or cellular structure of the liver, lungs, and spleens between the boanmycin-treated groups and the vehicle-treated groups, indicating that boanmycin has minimal side effects on these organs (Supplementary Fig. 3F-H). Furthermore, we obtained six clinical samples from MM patients, including three individuals (patients 1, 2, and 3) who experienced relapse and exhibited resistance to bortezomib. Then, cell viability assays were performed on patient-derived bone marrow mononuclear cells (BMMCs). The results showed a favorable inhibitory effect of boanmycin on BMMCs (Fig. 6F and Supplementary Fig. 3I). Overall, boanmycin effectively suppressed MM cells in mouse xenograft models, irrespective of their sensitivity or resistance to bortezomib. In addition, boanmycin also inhibited BMMCs derived from relapsed patients.

Discussion

Multiple myeloma is a heterogeneous hematological malignancy characterized by a dismal prognosis [1]. Resistance to proteasome inhibitors presents tremendous challenges in patient management. The mechanisms of drug resistance mainly include mutations in proteasome subunits, upregulation of prosurvival signaling and multidrug efflux transporters, and alterations in the bone marrow microenvironment [21]. Currently, MM remains incurable, and patients eventually succumb to the disease and its complications [22]. Therefore, developing additional therapeutic options, including novel compounds, is essential for improving the outcomes and quality of life of MM patients.

Boanmycin has demonstrated significant inhibitory effects on various malignancies [10]. However, its effectiveness in treating MM has not been previously reported. The administration of bleomycin to MM patients with malignant pericardial effusion implies the potential utility of other bleomycin derivatives in MM therapy [23]. Boanmycin, owing to its lower lung toxicity and bone marrow inhibition than bleomycin does, has potential for application in the treatment of MM [9, 10]. Our study revealed that boanmycin effectively inhibited the proliferation and colony formation of both BTZ-sensitive and BTZ-resistant MM cells (Figs. 1 and 3). The efficacy of combining bleomycin with adriamycin, vinblastine, and dacarbazine in improving survival rates among Hodgkin lymphoma patients has been substantiated [24]. However, few studies have explored the potential benefits of combining bleomycin derivatives with BTZ for the treatment of multiple myeloma. Our findings first demonstrated that boanmycin enhanced the inhibitory effect of BTZ on MM cells (Fig. 2A). MM cells treated with the combination of boanmycin and BTZ exhibited greater apoptosis than MM cells treated with either drug alone (Fig. 2B and C). Boanmycin treatment also increased cleaved caspase 3, cleaved caspase 7, and cleaved PARP protein levels (Figs. 1G and 3E), suggesting the activation of a canonical apoptosis signaling pathway.

Bleomycin and its derivatives are believed to induce single- and double-strand DNA breaks and lead to genomic instability [29]. Our study demonstrated that boanmycin induces an increase in γ-H2AX protein levels and a decrease in pathways related to DNA replication, mitotic spindle organization, and cell cycle regulation, suggesting the induction of DNA damage (Fig. 4E and Supplementary Fig. 2D, E). Additionally, both boanmycin and bleomycin have been shown to induce cell senescence in certain cell lines, indicating a potential common cytotoxic mechanism [25, 26]. However, boanmycin exhibits lower levels of lung toxicity and bone marrow suppression than bleomycin, potentially due to its different amino-terminal residues [27, 28]. Furthermore, boanmycin has more positively charged tails than bleomycin, potentially improving its cellular uptake [29]. Bleomycin interacts with proteins and impedes autophagy [30], which suggests that boanmycin may also have additional effects on pathways in addition to DNA targeting.

Researchers are exploring other potential ways to overcome the therapeutic resistance of MM patients. For example, the BCL-2 inhibitor venetoclax, in combination with dexamethasone, is being assessed for patients with relapsed/refractory multiple myeloma [31]. Targeting the NF-κB signaling pathway in MM has manifested significant antitumor effects [32]. The excessive production of monoclonal proteins leads to MM cells relying on the unfolded protein response (UPR) for survival, which increases their vulnerability to proteotoxicity [33]. Therefore, disrupting ER functions could promote the activity of proteasome inhibitors or resensitize drug-resistant patients [34]. Our findings indicate that boanmycin treatment resulted in the upregulation of pathways associated with ER function and the calcium signaling pathway (Fig. 5A). Transmission electron microscopy (TEM) revealed an irregular arrangement and elongation of the ER in cells treated with boanmycin (Fig. 5C). Additionally, ER-Tracker staining revealed a significant increase in probe signaling following boanmycin treatment (Fig. 5D and E). The ER serves as the primary intracellular store for Ca^{2+} and plays a crucial role in maintaining Ca^{2+} homeostasis [14]. Our data indicated that boanmycin treatment significantly increased the cytoplasmic Ca^{2+} level (Fig. 5F and G). These results suggest that the functional impairment of the ER is induced by boanmycin. We demonstrated that the combination of boanmycin

and BTZ led to an increase in the expression of the ER stress-related gene CHOP (Fig. 5B). However, boanmycin alone resulted in only a slight increase in CHOP gene expression, indicating the need for further evidence to determine whether boanmycin can induce ER stress. The P53 signaling pathway is known to play a crucial role in ER function [35, 36]. Our results revealed that boanmycin could enhance P53 signaling (Supplementary Fig. 2E). Additionally, boanmycin also activated the JNK signaling pathway (Supplementary Fig. 2D), which is a downstream target of ER stress [37, 38]. Thus, our findings indicate that boanmycin induces endoplasmic reticulum functional impairment, resulting in JNK activation and subsequent initiation of mitochondria-mediated apoptosis in multiple myeloma cells (Fig. 6G).

In this study, we examined the impact of boanmycin on MM cells in vivo utilizing BALB/c-nu and NOD-SCID mouse xenograft models. Our findings indicated that a dose of 10 mg/kg boanmycin effectively suppressed tumor growth without adversely affecting the motor activity or feeding behavior of the mice (Fig. 6). Although bleomycin and its derivatives demonstrate potent antitumor effects, their clinical utility is limited by the occurrence of side effects such as pulmonary fibrosis and neuronal impairments [39]. In our study, histological examination using HE staining did not reveal any notable alterations in the tissue or cellular architecture of the livers, lungs, and spleens of the mice treated with boanmycin compared with those in the vehicle groups (Supplementary Fig. 3F, G, H). These findings suggest that the administration of this particular dosage and route of boanmycin has limited adverse effects on these organs. Nevertheless, the effects of boanmycin on the nervous and digestive systems warrant further investigation. Our findings indicated that the body weights of the mice that were administered boanmycin were generally lower than those of the vehicle-treated groups, although this difference did not reach statistical significance (Fig. 6E; Supplementary Fig. 3D).

The inhibitory effects of boanmycin on patient-derived mononuclear cells were confirmed in our study. Boanmycin had favorable inhibitory effects on patient-derived BMMCs from a cohort of 6 MM patients, including 3 individuals who experienced relapse and exhibited resistance to BTZ (Fig. 6F and Supplementary Fig. 3I). However, further validation in a larger sample size of patient cohorts is imperative. Clinical trials evaluating the efficacy of boanmycin in MM patients have not yet been conducted. Nevertheless, our findings suggest that boanmycin may be a potential alternative treatment option for MM, particularly in patients who are resistant to BTZ.

Conclusion

Collectively, our data demonstrate that boanmycin disrupts the cell cycle and induces apoptosis by causing DNA damage and functional impairment of the ER in MM cells (Fig. 6G). Notably, boanmycin effectively inhibited the growth of BTZ-resistant MM cells. Additionally, our results emphasize the substantial inhibition of MM cell growth by boanmycin in mouse xenograft models and patient-derived BMMCs. These findings suggest the promising potential of boanmycin for the treatment of MM.

Abbreviations

BTZ	Bortezomib
MM	Multiple myeloma
ER	Endoplasmic reticulum
BMMCs	Bone marrow mononuclear cells
TEM	Transmission electron microscopy
CFSE	Carboxyfluorescein succinimidyl ester
CCK8	Cell counting kit 8

Supplementary Information

The online version contains supplementary material available at https://doi.org/10.1186/s13062-024-00590-y.

Supplementary Material 1

Supplementary Material 2

Acknowledgements

We thank Jilin AoDong Pharmaceutical Group Company for providing the boanmycin.

Author contributions

JXW and FQT contributed to the study conception and design, data analysis and interpretation of the data; JXW drafted the manuscript, and WZ and YL revised the manuscript. JXW, LZ, PWZ, LWY, JJ and XHC conducted the experiments and data acquisition. FQT, YL, and JXW provided financial support. All authors agree to submit this manuscript.

Funding

This work was supported by grants from the National Natural Science Foundation of China (No. 82200181 to JXW), the Natural Science Foundation of Shenzhen (No. JCYJ20230807141759001, JCYJ20220530162204009 and JCYJ20180306170407292 to FQT), the Special Fund Project for Economic and Technological Development of Longgang District, Shenzhen (No. LGKCYLWS2021000008 to FQT), the School and Hospital Joint Fund of the Second Affiliated Hospital of Chinese University of Hong Kong, Shenzhen (No. YXLH2203 to JXW), the Natural Science Foundation of Guangdong Province (No. 2022A1515010128 to YL) and the Pearl River Talent Program (No. 2021QN02Y438 to YL).

Data availability

No datasets were generated or analysed during the current study.

Declarations

Ethics approval and consent to participate

Bone marrow mononuclear cells (BMMCs) were collected from MM patients with approval from the Institute Research Ethics Committee (No. 2024014) of The Second Affiliated Hospital of the Chinese University of Hong Kong (Shenzhen), following the Helsinki Declaration. The animal experiments were approved by the Institutional Animal Care and Use Committee of The Chinese University of Hong Kong (Shenzhen) (No. CUHKSZ-AE2021011), following the WMA statement on animal use in biomedical research.

Consent for publication
Not applicable.

Competing interests
The authors declare no competing interests.

Author details
[1]Department of Hematology, The Second Affiliated Hospital, School of Medicine, The Chinese University of Hong Kong, Shenzhen & Longgang District People's Hospital of Shenzhen, Shenzhen 518172, China
[2]Guangdong Key Laboratory for Biomedical Measurements and Ultrasound Imaging, School of Biomedical Engineering, National-Regional Key Technology Engineering Laboratory for Medical Ultrasound, Shenzhen University Medical School, Shenzhen 518060, China
[3]Department of Pathology Technique, Guangdong Medical University, No.1 Xincheng Road, Dongguan, Guangdong Province 523808, China
[4]Department of Hematology, The Third Affiliated Hospital, Institute of Hematology, Sun Yat-sen University, Guangzhou 510630, China
[5]School of Medicine, The Chinese University of Hong Kong, Shenzhen, Guangdong 518172, China

Received: 1 July 2024 / Accepted: 26 December 2024
Published online: 06 January 2025

References

1. Silberstein J, Tuchman S, Grant SJ. What Is Multiple Myeloma? JAMA. 2022;327(5):497.
2. van de Donk N, Pawlyn C, Yong KL. Multiple myeloma. Lancet. 2021;397(10272):410–27.
3. Braggio E, Kortum KM, Stewart AK. SnapShot: multiple myeloma. Cancer Cell. 2015;28(5):678–e1.
4. Scott K, Hayden PJ, Will A, Wheatley K, Coyne I. Bortezomib for the treatment of multiple myeloma. Cochrane Database Syst Rev. 2016;4(4):CD010816.
5. Zheng Z, Fan S, Zheng J, Huang W, Gasparetto C, Chao NJ, et al. Inhibition of thioredoxin activates mitophagy and overcomes adaptive bortezomib resistance in multiple myeloma. J Hematol Oncol. 2018;11(1):29.
6. Gandolfi S, Laubach JP, Hideshima T, Chauhan D, Anderson KC, Richardson PG. The proteasome and proteasome inhibitors in multiple myeloma. Cancer Metastasis Rev. 2017;36(4):561–84.
7. Deng YC, Zhen YS, Zheng S, Xue YC. Activity of boanmycin against colorectal cancer. World J Gastroenterol. 2001;7(1):93–7.
8. Ding W, Li Y, Hou X, Li G. Bleomycin A6-loaded anionic liposomes with in situ gel as a new antitumoral drug delivery system. Drug Deliv. 2016;23(1):88–94.
9. Feng F, Zhou L, Mang Z, Liu H, Sun Y. [Phase I clinical study of a new anticancer drug boanmycin]. Zhongguo Yi Xue Ke Xue Yuan Xue Bao. 1996;18(2):143–6.
10. Feng F, Zhou L. [Phase II clinical study of a new anticancer drug boanmycin]. Zhongguo Yi Xue Ke Xue Yuan Xue Bao. 1999;21(4):247–51.
11. Wang ZH, Ding WM, Hu XD, Li M, Xu HZ, Qian LX. Effect of peritumoral injection of boanmycin hydrochloride within temperature-sensitive in situ gel using Hep-G2 hepatoma nude mice model. Chin Med J (Engl). 2012;125(23):4291–5.
12. Schwarz DS, Blower MD. The endoplasmic reticulum: structure, function and response to cellular signaling. Cell Mol Life Sci. 2016;73(1):79–94.
13. Westrate LM, Lee JE, Prinz WA, Voeltz GK. Form follows function: the importance of endoplasmic reticulum shape. Annu Rev Biochem. 2015;84:791–811.
14. Zheng S, Wang X, Zhao D, Liu H, Hu Y. Calcium homeostasis and cancer: insights from endoplasmic reticulum-centered organelle communications. Trends Cell Biol. 2023;33(4):312–23.
15. Oakes SA, Papa FR. The role of endoplasmic reticulum stress in human pathology. Annu Rev Pathol. 2015;10:173–94.
16. Chen X, Cubillos-Ruiz JR. Endoplasmic reticulum stress signals in the tumour and its microenvironment. Nat Rev Cancer. 2021;21(2):71–88.
17. Xiong S, Chng WJ, Zhou J. Crosstalk between endoplasmic reticulum stress and oxidative stress: a dynamic duo in multiple myeloma. Cell Mol Life Sci. 2021;78(8):3883–906.
18. Yeung M, Hurren R, Nemr C, Wang X, Hershenfeld S, Gronda M, et al. Mitochondrial DNA damage by bleomycin induces AML cell death. Apoptosis. 2015;20(6):811–20.
19. Tang H, Yang XP. [Effect of boanmycin on apoptosis and cell cycle of human esophageal cancer(Eca-109) cells]. Ai Zheng. 2002;21(8):855–9.
20. Ashby MC, Tepikin AV. ER calcium and the functions of intracellular organelles. Semin Cell Dev Biol. 2001;12(1):11–7.
21. Niewerth D, Jansen G, Assaraf YG, Zweegman S, Kaspers GJ, Cloos J. Molecular basis of resistance to proteasome inhibitors in hematological malignancies. Drug Resist Updat. 2015;18:18–35.
22. Joseph NS, Kaufman JL, Dhodapkar MV, Hofmeister CC, Almaula DK, Heffner LT, et al. Long-term Follow-Up results of Lenalidomide, Bortezomib, and Dexamethasone Induction Therapy and Risk-Adapted Maintenance Approach in newly diagnosed multiple myeloma. J Clin Oncol. 2020;38(17):1928–37.
23. Mitchell MA, Horneffer MD, Standiford TJ. Multiple myeloma complicated by restrictive cardiomyopathy and cardiac tamponade. Chest. 1993;103(3):946–7.
24. Stephens DM, Boucher K, Kander E, Parikh SA, Parry EM, Shadman M, et al. Hodgkin lymphoma arising in patients with chronic lymphocytic leukemia: outcomes from a large multi-center collaboration. Haematologica. 2021;106(11):2845–52.
25. Chen F, Zhao W, Du C, Chen Z, Du J, Zhou M. Bleomycin induces senescence and repression of DNA repair via downregulation of Rad51. Mol Med. 2024;30(1):54.
26. Chen P, Guo H, Chen J, Fu Y. The chemotherapeutic drug boanmycin induces cell senescence and senescence-associated secretory phenotype factors, thus acquiring the potential to remodel the tumor microenvironment. Anticancer Drugs. 2016;27(2):84–8.
27. Kong J, Yi L, Xiong Y, Huang Y, Yang D, Yan X, et al. The discovery and development of microbial bleomycin analogues. Appl Microbiol Biotechnol. 2018;102(16):6791–8.
28. Ma Q, Xu Z, Schroeder BR, Sun W, Wei F, Hashimoto S, et al. Biochemical evaluation of a 108-member deglycobleomycin library: viability of a selection strategy for identifying bleomycin analogues with altered properties. J Am Chem Soc. 2007;129(41):12439–52.
29. Chen J, Stubbe J. Bleomycins: towards better therapeutics. Nat Rev Cancer. 2005;5(2):102–12.
30. Wang K, Zhang T, Lei Y, Li X, Jiang J, Lan J, et al. Identification of ANXA2 (annexin A2) as a specific bleomycin target to induce pulmonary fibrosis by impeding TFEB-mediated autophagic flux. Autophagy. 2018;14(2):269–82.
31. Kaufman JL, Gasparetto C, Schjesvold FH, Moreau P, Touzeau C, Facon T, et al. Targeting BCL-2 with venetoclax and dexamethasone in patients with relapsed/refractory t(11;14) multiple myeloma. Am J Hematol. 2021;96(4):418–27.
32. Brunelli D, Tavecchio M, Falcioni C, Frapolli R, Erba E, Iori R, et al. The isothiocyanate produced from glucomoringin inhibits NF-kB and reduces myeloma growth in nude mice in vivo. Biochem Pharmacol. 2010;79(8):1141–8.
33. Nikesitch N, Lee JM, Ling S, Roberts TL. Endoplasmic reticulum stress in the development of multiple myeloma and drug resistance. Clin Transl Immunol. 2018;7(1):e1007.
34. Dong X, Liao Y, Liu N, Hua X, Cai J, Liu J, et al. Combined therapeutic effects of bortezomib and anacardic acid on multiple myeloma cells via activation of the endoplasmic reticulum stress response. Mol Med Rep. 2016;14(3):2679–84.
35. Chen Q, Thompson J, Hu Y, Das A, Lesnefsky EJ. Cardiac specific knockout of p53 decreases ER stress-Induced mitochondrial damage. Front Cardiovasc Med. 2019;6:10.
36. Lopez I, Tournillon AS, Prado Martins R, Karakostis K, Malbert-Colas L, Nylander K, et al. p53-mediated suppression of BiP triggers BIK-induced apoptosis during prolonged endoplasmic reticulum stress. Cell Death Differ. 2017;24(10):1717–29.
37. Chen YY, Sun LQ, Wang BA, Zou XM, Mu YM, Lu JM. Palmitate induces autophagy in pancreatic beta-cells via endoplasmic reticulum stress and its downstream JNK pathway. Int J Mol Med. 2013;32(6):1401–6.
38. Lee H, Park MT, Choi BH, Oh ET, Song MJ, Lee J, et al. Endoplasmic reticulum stress-induced JNK activation is a critical event leading to mitochondria-mediated cell death caused by beta-lapachone treatment. PLoS ONE. 2011;6(6):e21533.

39. Della Latta V, Cecchettini A, Del Ry S, Morales MA. Bleomycin in the setting of lung fibrosis induction: from biological mechanisms to counteractions. Pharmacol Res. 2015;97:122–30.

Publisher's note